LA-UR-21-24350
Approved for public release; distribution is unlimited.

Title: (U) Validation and Optimization of a 1-Dimensional Quasi-Isentropic Compression Model Using a Functionally Graded Material Flyer Plate

Author(s): Gomez, Jaime A.

Intended for: Report

Issued: 2021-05-05

# (U) Validation and Optimization of a 1-Dimensional Quasi-Isentropic Compression Model Using a Functionally Graded Material Flyer Plate

Jaime Gomez[1]

[1]XTD-PRI, Los Alamos National Laboratory

Date: May 4, 2021

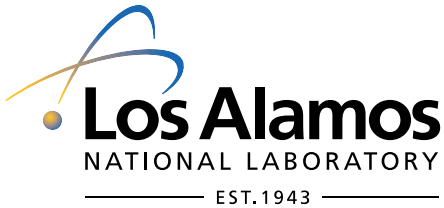


# Contents



# List of Figures

# List of Tables

# 1 Introduction

The fields studying highly compressed materials have been around for many years. These fields have given birth to better understandings of the solar fusion cycle and the liquid-metallic core of Jupiter. The highest pressures achieved have been at the National Ignition Facility (NIF) and more recently, the Z-Machine.

One method to achieve higher levels of compression is to use quasi-isentropic (QI) compression[6, 7, 8]. In practice, this means minimizing the amount of temperature increase of the target material. In their paper, J.H. Nguyen et. al. manufactured a functionally graded material (FGM) in order to help them achieve QI compression [6].

The aim of the study described in this paper is to validate a 1-dimensional (1D) FLAG[3] model that uses an FGM flyer to compress a copper (Cu) target. Once validated, the density/composition profile of the FGM is varied and optimized using Markov Chain Monte Carlo, specifically using a Metropolis-Hastings algorithm to find the optimal FGM profile that minimizes the temperature increase in the copper.

# 2 Experimental Description

The model was meant to first reproduce the results found in [6, 7, 8] in order to validate a starting point for future studies. The experimental apparatus described in Ref. [6] mentions a 1 centimeter (cm) thick lithium-fluoride (LiF) VISAR window; through which velocimetry information was collected. The window is abut to a 0.5 [cm] thick layer of Cu, which is the target material meant to be compressed. Nguyen et. al. used a gas gun to project the FGM at several velocities (1.0 and 1.2 $\left[\frac{\text{km}}{\text{s}}\right]$) towards the Cu target[6].

The functionally graded material itself consists of 35 individual layers. Each layer is 200 $[\mu m]$ thick, resulting in a total thickness of 0.7 [cm]. A cartoon depicting the experimental layout is shown below in Figure 1.

The low impedance layers are made up of a porous foam (polystyrene)[5]. The modeling choices for these foams will be discussed in the subsequent sections. The higher density layers are modeled as a mixture of foam-aluminum (Al), and aluminum-tungsten (W). Reference [6] describe the layers as being powdered and mixed in the appropriate proportions to make the desired impedances, in the case of the foam and

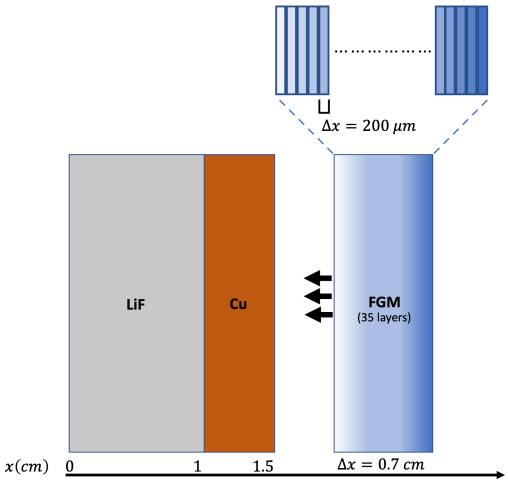


Figure 1: A cartoon showing the typical experimental setup found in Ref. [6]. The FGM impactor is launched toward a stationary Cu target at velocities up to 4.5 $\left[\frac{\text{km}}{\text{s}}\right]$.

Al mixture, the powered Al is said to be deposited on a foam matrix.

Ray and Menon[7] describe a similar modeling attempt whereby a linear, quadratic, cubic, and exponential density profile are used. This study uses a quadratic density profile of the form

$$\rho = \rho_1 + a\,(x - x_1)^2\,, \tag{1}$$

where $\rho_1 = 0.1\ \left[\frac{\text{g}}{\text{cm}^3}\right]$, and $a = 32.22\ \left[\frac{\text{g}}{\text{cm}^5}\right]$. The density profile of the modeled FGM can be seen in Figure 2. Similar to Ref. [7], the density ranges from 0.1 $\left[\frac{\text{g}}{\text{cm}^3}\right]$to 15 $\left[\frac{\text{g}}{\text{cm}^3}\right]$.

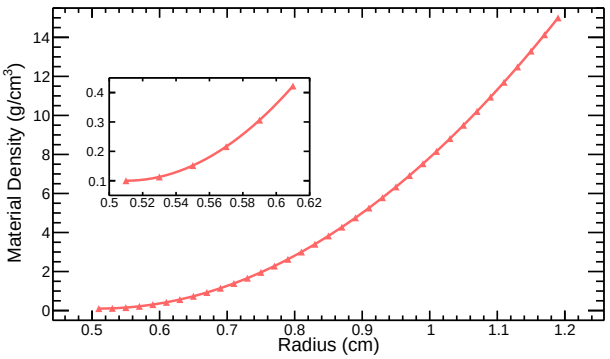


Figure 2: The starting density profile for the FGM, taken from Ref. [7].

# 3 Modeling

The model for the experiment is made in FLAG[3], an arbitrary Lagrangian-Eulerian multi-physics code. This code allows a user to have access to a wide variety of different modeling choices as the modeler deems them appropriate.

## 3.1 Artificial Viscosity

An incoming shock has a thickness of a few molecular mean free paths. As such, it is impractical to resolve a macroscopic-sized model to such a scale. This underresolution creates a discontinuity between regions where there is an abrupt change in velocity, density, energy, and pressure. One well established way of calculating hydrodynamic evolution in a shocked environment is the introduction of artificial viscosity.

The concept of artificial viscosity was originally introduced by von Neumann and Richtmyer[9]. This method introduces a 'viscosity-like' term that will spread the thickness of any shock over several cells in a computational mesh. Where P, pressure, usually appears in the momentum and energy equations, P+Q, appears [3]. This substitution removes the discontinuities in the solutions. As a result, the standard numerical methods can be used to calculate solutions to simulate shock propagation through all of the materials in the problem.

## 3.2 Equation of State

If the Hugoniot of a material is known, a Mie-Grüneisen EOS can be used to calculate the material state in a condition off the principal Hugoniot[2, 4]. A Mie-Grüneisen EOS has the form:

$$P - P_H = \gamma\rho\left(E - E_H\right), \tag{2}$$

where $P$ and $E$ are the pressure and energy (respectively) in the material at the state of interest, and the subscript $H$, refers to the standard Hugoniot state. The $\gamma$, and $\rho$ are the Grüneisen gamma and the shocked compressed density respectively. The Hugoniot equations for conservation of mass, momentum, and energy are:

$$\rho_0 U_s = \rho\left(U_s - U_p\right), \tag{3}$$

$$P_H = \rho_0 U_s U_P, \tag{4}$$

$$E_H = E_0 + \frac{1}{2}P_H\left(\frac{1}{\rho_0} - \frac{1}{\rho}\right); \tag{5}$$

where $U_s$, $U_p$ are the shock and particle velocities respectively, and $E_0$,and $\rho_0$ are the energy and density at ambient conditions. Experimental data suggests that shock velocity is linearly related to particle velocity such that

$$U_s = c_0 + sU_p, \tag{6}$$

where $c_0$ is the bulk sound speed at constant entropy, given by $c_0^2 = \left(\frac{\partial P}{\partial \rho}\right)_S$. The slope, $s$, is related to the pressure derivative of the isentropic bulk modulus at ambient pressure[5]. These values are typically measured experimentally. The parameters used in this model are taken from Meyers[5], they are shown in Table 1.

| | **Foam** | **Aluminum** | **Tungsten** |
|---|---|---|---|
| **Parameter** | | | |
| $\rho_0$ $\left[\frac{\mathrm{g}}{\mathrm{cm}^3}\right]$ | 1.04 | 2.750 | 19.22 |
| $c_v$ $\left[\frac{\mathrm{J}}{\mathrm{g-K}}\right]$ | 1.2 | 0.89 | 0.13 |
| $C_0$ $\left[\frac{\mathrm{cm}}{\mu\mathrm{s}}\right]$ | 0.275 | 0.5328 | 0.403 |
| $s$ | 1.32 | 1.338 | 1.24 |
| $\gamma_0$ | 1.2 | 2 | 1.8 |

Table 1: The Mie-Grüneisen parameters for a mixed EOS composed of the above materials[5].

In the FLAG model, each FGM layer that is a mixture of foam-Al, and Al-W is treated as a composite material in the following way [5]:

$$\rho_0 = \sum_i m_i \rho_{0_i} \tag{7}$$

$$c = \sum_i m_i c_i \tag{8}$$

$$s = \sum_i m_i s_i \tag{9}$$

where $m_i$ represents the mass fraction of each material in the composite.

In the case of this study, we have the density profile shown in Fig. 2, and the initial density of each of the 35 layers is set to be constant. That initial density of each layer is found by taking the radius value at the center of each layer and finding the density in the function given in Eq. 1. With the knowledge of the densities, solving for the mass fraction of each material, in each layer becomes:

$$\chi_1 = \frac{(\rho_1 \cdot (\rho_2 - \rho_{\text{Composite}}))}{(\rho_{\text{Composite}} \cdot (\rho_2 - \rho_1))}, \tag{10}$$

$$\chi_2 = 1 - \chi_1, \tag{11}$$

where $\chi$ and $\rho$ are the mass fractions and densities, with subscripts 1 and 2 representing material 1 and material 2, and $\rho_{\text{Composite}}$ is the known density for the layer given by Eq. 1. The initial mass fractions densities and other parameters used in the model are found in Appendix A.

## 3.3 Underdense Foam

In Meyers[5], the density of polystyrene is tabulated as 1.04 $\left[\frac{\text{g}}{\text{cm}^3}\right]$. In practice, for the first layer to have 0.1 $\left[\frac{\text{g}}{\text{cm}^3}\right]$, the foam would be made porous. In this model, three different approaches were attempted in order to capture the physics of having a porous foam.

### 3.3.1 Equation of State with Ramp

One of the most commonly used methods to model porous materials prior to their becoming solid is the use of a ramp. An example of such a "crushing out" of porosity is seen below in Figure 3.

It should be noted that a ramp need not consist of two linear segments. A ramp allows the simulation to model the pressure inside the material in the following way:

$$P_{\text{ramp}}(\rho) = \begin{cases} 0 & \rho < \rho_0 \\ a\left(\frac{\rho}{\rho_0} - 1\right) & \rho_0 \le \rho < \rho_0 \frac{a-bc}{a-b} \\ b\left(\frac{\rho}{\rho_0} - c\right) & \rho_0 \frac{a-bc}{a-b} \le \rho < \rho_1 \end{cases}, \tag{12}$$

where $a$ is the bulk modulus of ramp$_1$, $b$ is the bulk modulus of ramp$_2$, $c$ is called the ramp parameter,

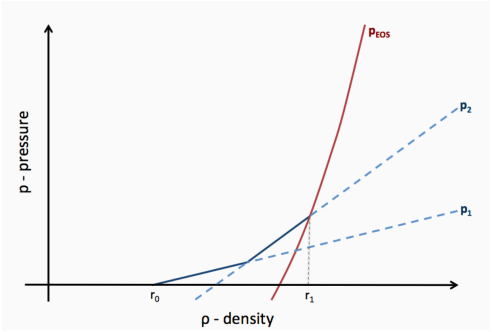


Figure 3: Modeling crushing of a porous material with a bi-linear ramp. The first linear segment captures the regime in which the porosity is crushing out but the bulk material is not compressing. The second linear segment captures the regime in which porosity continues to crush out and the bulk material is also compressing. The EOS captures the regime in which all porosity has been crushed out and the bulk material is solely responsible for any density change[3].

and $\rho_0$ is the reference density for the material. Once the underdense material is equal to $\rho_1$, which is where the ramp pressure, and the pressure of a tabulated Hugoniot are the same, the material will default back to using the standard EOS. This is equivalent to all of the pores being crushed out.

### 3.3.2 P-$\alpha$ Model

Another, more modern, way to model underdense material is the use of a P-$\alpha$ model[1]. The P-$\alpha$ model consists of seperating the porous volume material into two parts: pore collapse portion, and compression of the matrix material, in this case polystyrene. This separation is brought about by defining the $\alpha$ term:

$$\alpha \equiv \frac{\rho_0}{\rho}, \tag{13}$$

where $\rho_0$ is the bulk density of the matrix material when not porous, and $\rho$ is the bulk density of the porous material. In Ref. [1], Carrol and Holt explicity write the EOS of the porous material as:

$$P = \frac{1}{\alpha} P_s\left(\rho_s, E_s\right) = \frac{1}{\alpha} P_s\left(\alpha\rho, E\right), \tag{14}$$

where $P_s\left(\rho_s, E_s\right)$ represents the pressure of the non-porous foam. A noteable feature of this model is that the pressure depends on the density of the foam. The pores are modeled simply as voids which means that the surface energy of the pores is neglected. This is a reasonable approximation in most applications and once the material again has been crushed out, it returns to using the Hugoniot prescribed by the Mie-Grüneisen formulation.

#### 3.3.3 Scaling Ratio

The last modeling method used to simulate the porous foam in the inner most layers is the use of a scaling ratio. This entails simply taking a ratio:

$$\text{s.r.} = \frac{\rho_{\text{ref}}}{\rho}, \tag{15}$$

where $\rho_{\text{ref}}$ is the density of the material in normal conditions, and $\rho$ is the density of the porous foam. The scaling ratio simply scales the Hugoniot, and in doing so the thermodynamic properties should remain consistent with the material under normal conditions. This approximation fails if the density of the porous material is significantly different than the nominal density. In the case of this problem the starting density of the lowest impedance FGM is 10% the nominal.

#### Comparison

Below in Figure 4, we see that at early times the three different methods for modeling the FGM are in complete agreement. The difference manifests itself at around 2.5$\mu$s with the rarefaction wave making its way back to the FGM layers.

Similar behavior is observed in Figure 5. Once the rarefaction wave has propagated through the entirety of the FGM the results become divergent. But prior to this the results appear to agree.

Comparison to previous simulations and data will be shown in Section 4.

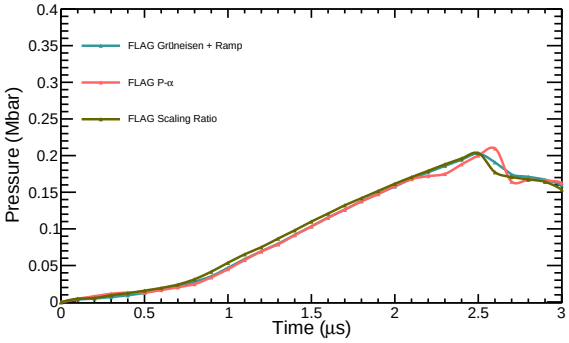


Figure 4: Pressure applied at the flyer-target interface as a function of time for the three different treatments of the FGM mentioned in Section 3. They are Grüneisen + Ramp, P-$\alpha$, and Scaling Ratio.

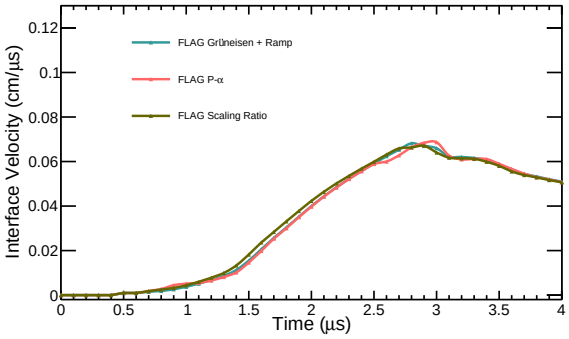


Figure 5: Target-window interface velocity for the three different treatments of the FGM mentioned in Section 3. They are Grüneisen + Ramp, P-$\alpha$, and Scaling Ratio.

# 4 Results

## 4.1 Comparison to Simulation [7]

In their paper, Ray and Menon[7] showed the pressure applied to the target from the flyer as a function of time. In Figure 6, I compare the pressure evolution from FLAG with the results from Ref. [7].

It can be seen, that while the applied pressure never reaches a peak as high as Ray and Menon; the time evolution looks qualitatively similar.

In the same manuscript, Ray and Menon show the measured velocity of at the LiF window and Cu target interface. The velocimetery data were shown for various FGM density profiles (linear, quadratic, cubic, log, etc.). In Figure 7, it is shown that a reason-

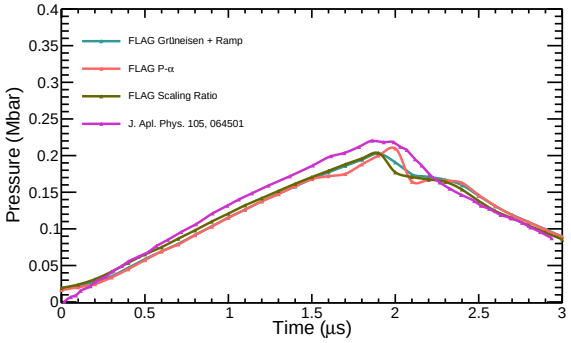


Figure 6: Simulated applied pressure data from FLAG (blue, red, green) compared to data from Ray and Menon[7] (purple). Qualitative agreement is observed despite the absolute peak pressures being different.

able agreement exists between the simulations from FLAG and the simulations of Ray and Menon.

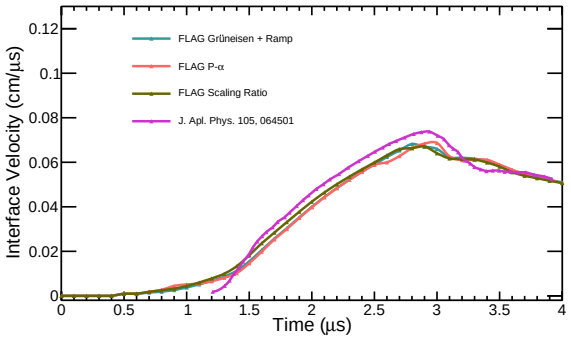


Figure 7: Simulated velocimetry data from FLAG (blue, red, green) compared to data from Ray and Menon[7] (purple). Qualitative agreement is observed despite the absolute peak velocities being different.

It should be noted that in their paper[7], Ray and Menon claim to have qualitatively good agreement between their velocimetry data and that shown in [6]. This qualitative agreement, it will be shown, is not true beyond early times. This is even when one considers that absolute simulation time is not as important as the shape of the pressure and velocity curves.

## 4.2 Comparison to Data [6]

Within reason, it is a fair statement to say that absolute timing when comparing simulation and data is not as important as overall time-evolving shape and magnitude of quantity of interest. As such, in Figure 8, and Figure 9, it can be seen that the shape and magnitude of the simulated velocimetry data does not agree with the results in Ref. [6]. While there are several, notable, features in both the data and simulation, in order to "match" the times between FLAG and the data, it has been elected to match to the initial rise of the speed of the target.

The times reported in Ref. [6] have not been altered, however an analyzer was written to check the derivitive of the curves shown in Figures 8 and 9 at early times (between 0.5 and 2.5 $\mu$s). Once the slope began to increase over the previous 10 data points, the algorithm would trigger and report a time for the data.The same procedure of locating the initial rise of the velocity was also preformed on the FLAG simulated output. With the time in the corresponding FLAG simulation now matched to the data, a direct comparison is now appropriate.This method of time-tying also proved robust when the reported times in the two datasets, 1.0 $\left[\frac{\text{km}}{\text{s}}\right]$, and 1.2 $\left[\frac{\text{km}}{\text{s}}\right]$ were found to have a time difference on their sharp rise of 0.5 $\mu$s. The exact same time shift was seen between the FLAG models where the flyer (FGM) was launched at 1.0 and 1.2 $\left[\frac{\text{km}}{\text{s}}\right]$.

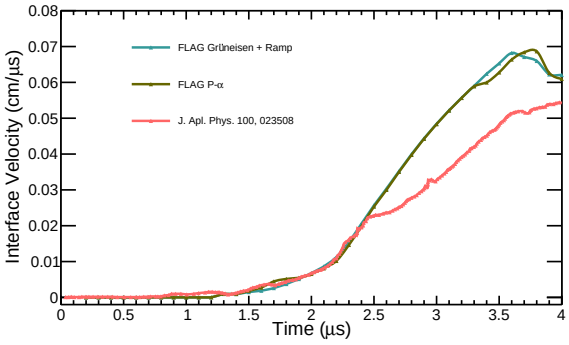


Figure 8: Comparison of FLAG-simulated velocimetry data at the window-target interface (blue, green) with an initial flyer velocity of 1.0 $\left[\frac{\text{km}}{\text{s}}\right]$. The simulated times were matched to the data times (plotted in salmon) matching derivitives at early times, 0.5 - 2.5 $\mu$s.

Despite being confident in the procedure, the results show a much different velocimetry profile from 2.5 $\mu$s onward in the simulation time. The FLAG model shows a much higher acceleration than the data. The reason for this difference will be investigated.

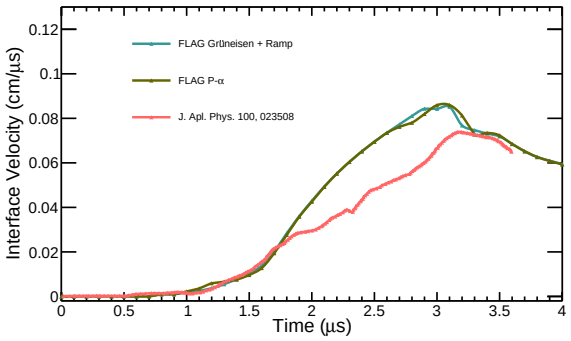


Figure 9: Comparison of FLAG-simulated velocimetry data at the window-target interface (blue, green) with an initial flyer velocity of 1.2 $\left[\frac{\text{km}}{\text{s}}\right]$. The simulated times were matched to the data times (plotted in salmon) matching derivitives at early times, 0.5 - 2.5 $\mu$s.

### 4.3 Optimization of the Density Profile of the FGM

In order to achieve the maximum QI compression, a Markov-Chain Monte Carlo (MCMC) program was used to test different density profiles. This would allow the computer to search for an optimized density profile in whatever arbitrary spline shape it discovers, instead of constraining the spline to a simple quadratic. Below in Figure 10, is the result of $10^4$ iterations of such an optimizer. One can see that the quadratic spline used initially (salmon curve), has not been changed drastically (purple points).

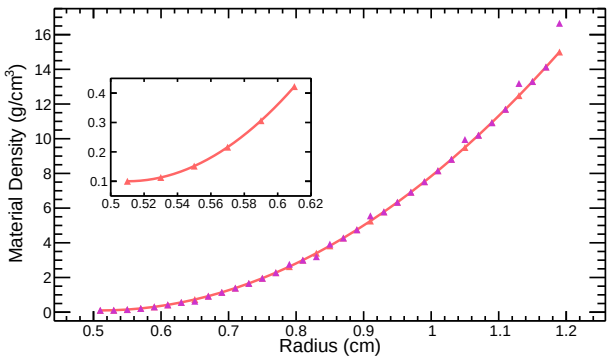


Figure 10: The plotted curve (salmon), is the same curve plotted in Fig. 2. The purple points overlayed the curve are the result of $10^4$ iterations of a Markov-Chain Monte Carlo algorithm that sampled different densities. One can see that while there is some deviation, the quadratic curve is close to already optimized. A similar result can also be found in Ref.[8].

Given more iterations, this profile could change even further from a quadratic spline, but as Ray and Menon[8] showed, the quadratic density profile seems to be close to optimal for this problem.

In addition to achieving better compression from a different density profile, Ray and Menon[8] also tried different layer thickness, as well as different numbers of layers. To truly find the optimal profile, one would have to preform multi-variate MCMC studies. This will likely be the subject of future exploratory efforts.

## 5 Conclusions

Functionally graded materials provide a unique opportunity to achieve higher levels of target compression thanks to the quasi-isentropic nature of that compression. A 1-dimensional model was created using FLAG to compare simulations to other published results [7, 8] and also published data [6]. These comparisons were done using three different methods for modeling underdense, porous foams. Comparisons to previous simulated results show a qualitative agreement while comparisons to actual data show wide discrepancies. A Markov-Chain Monte Carlo procedure was written and tested to demonstrate the ability to optimize the density profile of the FGM. A multivariate study of density, layer thickness, and number of layers could prove beneficial to further increase compression of the copper target.

## Acknowledgements

I first wanted to thank Cory Ahrens, whose patience with this project has been put to the test but who really helped in ways beyond the intellectual. Second, a special acknowledgement to Chris Malone, Miles Buechler, and Jim Hill; all three of you really helped me understand the necessary nodes inside of FLAG to get this project done, I could not have done it without you. Thank you to Donald Sandoval for the enlightening talks about different modeling methods. I lastly wanted to thank the XTD leadership team for the accomodations and support to allow me to finish this manuscript.

## References

[1] Michael Carroll and Albert C. Holt. Suggested Modification of the P-$\alpha$ Model for Porous Mate-

rials. *Journal of Applied Physics*, 43(2):759–761, 1972.

[2] E. Grüneisen. Theorie des festen Zustandes einatomiger Elemente. *Annalen der Physik*, 344(12):257–306, 1912.

[3] J. L. Hill. User's manual for flag version 3.7.0. *LA-CP*, 18(20066), 2018.

[4] R. Menikoff. Complete Mie-Grüneisen Equation of State". *LA-UR*, 12(22592), 2012.

[5] M.A. Meyers. *Dynamic Behavior of Materials*. Wiley-Interscience publication. Wiley, 1994.

[6] Jeffrey H. Nguyen, Daniel Orlikowski, Frederick H. Streitz, John A. Moriarty, and Neil C. Holmes. High-Pressure Tailored Compression: Controlled Thermodynamic Paths. *Journal of Applied Physics*, 100(2):023508, 2006.

[7] Aditi Ray and S. V. G. Menon. Quasi-isentropic Compression Using Functionally Graded Materials in Gas Gun and Explosive Driven Systems. *Journal of Applied Physics*, 105(6):064501, 2009.

[8] Aditi Ray and S. V. G. Menon. Hydrodynamic Simulation and Thermodynamic Characterization of Functionally Graded Material Induced Isentropic Compression: Towards Optimum Density Profile". *Journal of Applied Physics*, 110(2):024905, 2011.

[9] J. von Neumann and R. Richtmyer. A Method for the Numerical Calculation of Hydrodynamic Shocks. *Journal of Applied Physics*, 21:232 – 237, 04 1950.

# A Initial Settings for FGM Layers

Table 2: Layer thickness, composition, and Mie-Grüneisen EOS parameters for each of the 35 FGM layers.

| **Layer** | **Inner Radius (cm)** | **Outer Radius (cm)** | $\chi_{\text{Foam}}$ | $\chi_{\text{Al}}$ | $\chi_{\text{W}}$ | $\rho_0 \left[\frac{\text{g}}{\text{cm}^3}\right]$ | $\gamma_0$ | $s$ | $C_0 \left[\frac{\text{cm}}{\mu\text{s}}\right]$ | $C_v \left[\frac{\text{J}}{\text{g}-\text{K}}\right]$ |
|---|---|---|---|---|---|---|---|---|---|---|
| 01 | 1.50 | 1.52 | 1.0 | 0.0000 | 0.0000 | 0.1000 | 1.1912 | 1.3172 | 0.2720 | 1.1947 |
| 02 | 1.52 | 1.54 | 1.0 | 0.0000 | 0.0000 | 0.1129 | 1.1923 | 1.3176 | 0.2724 | 1.1954 |
| 03 | 1.54 | 1.56 | 1.0 | 0.0000 | 0.0000 | 0.1516 | 1.1945 | 1.3183 | 0.2731 | 1.1967 |
| 04 | 1.56 | 1.58 | 1.0 | 0.0000 | 0.0000 | 0.2160 | 1.1964 | 1.3189 | 0.2738 | 1.1979 |
| 05 | 1.58 | 1.60 | 1.0 | 0.0000 | 0.0000 | 0.3062 | 1.1978 | 1.3193 | 0.2742 | 1.1987 |
| 06 | 1.60 | 1.62 | 1.0 | 0.0000 | 0.0000 | 0.4222 | 1.1986 | 1.3196 | 0.2745 | 1.1992 |
| 07 | 1.62 | 1.64 | 1.0 | 0.0000 | 0.0000 | 0.5640 | 1.1992 | 1.3198 | 0.2747 | 1.1995 |
| 08 | 1.64 | 1.66 | 1.0 | 0.0000 | 0.0000 | 0.7315 | 1.1996 | 1.3199 | 0.2749 | 1.1998 |
| 09 | 1.66 | 1.68 | 1.0 | 0.0000 | 0.0000 | 0.9248 | 1.1999 | 1.3200 | 0.2750 | 1.1999 |
| 10 | 1.68 | 1.70 | 0.8539 | 0.1461 | 0.0000 | 1.1439 | 1.3169 | 1.3226 | 0.3127 | 1.1547 |
| 11 | 1.70 | 1.72 | 0.5961 | 0.4039 | 0.0000 | 1.3888 | 1.5231 | 1.3274 | 0.3791 | 1.0748 |
| 12 | 1.72 | 1.74 | 0.3997 | 0.6003 | 0.0000 | 1.6594 | 1.6803 | 1.3308 | 0.4298 | 1.0139 |
| 13 | 1.74 | 1.76 | 0.2469 | 0.7531 | 0.0000 | 1.9559 | 1.8024 | 1.3336 | 0.4691 | 0.9666 |
| 14 | 1.76 | 1.78 | 0.1260 | 0.8740 | 0.0000 | 2.2781 | 1.8992 | 1.3357 | 0.5003 | 0.9291 |
| 15 | 1.78 | 1.80 | 0.0287 | 0.9713 | 0.0000 | 2.6261 | 1.9770 | 1.3375 | 0.5254 | 0.8989 |
| 16 | 1.80 | 1.82 | 0.0000 | 0.9028 | 0.0972 | 2.9998 | 1.9806 | 1.3285 | 0.5202 | 0.8161 |
| 17 | 1.82 | 1.84 | 0.0000 | 0.7771 | 0.2229 | 3.3993 | 1.9554 | 1.3162 | 0.5039 | 0.7206 |
| 18 | 1.84 | 1.86 | 0.0000 | 0.6721 | 0.3279 | 3.8246 | 1.9344 | 1.3059 | 0.4902 | 0.6408 |
| 19 | 1.86 | 1.88 | 0.0000 | 0.5836 | 0.4164 | 4.2757 | 1.9167 | 1.2972 | 0.4787 | 0.5735 |
| 20 | 1.88 | 1.90 | 0.0000 | 0.5083 | 0.4917 | 4.7526 | 1.9017 | 1.2898 | 0.4690 | 0.5163 |
| 21 | 1.90 | 1.92 | 0.0000 | 0.4437 | 0.5563 | 5.2552 | 1.8887 | 1.2835 | 0.4606 | 0.4672 |
| 22 | 1.92 | 1.94 | 0.0000 | 0.3879 | 0.6121 | 5.7836 | 1.8776 | 1.2780 | 0.4533 | 0.4248 |
| 23 | 1.94 | 1.96 | 0.0000 | 0.3394 | 0.6606 | 6.3378 | 1.8679 | 1.2733 | 0.4471 | 0.3879 |
| 24 | 1.96 | 1.98 | 0.0000 | 0.2969 | 0.7031 | 6.9178 | 1.8599 | 1.2691 | 0.4415 | 0.3557 |
| 25 | 2.98 | 2.00 | 0.0000 | 0.2596 | 0.7404 | 7.5235 | 1.8519 | 1.2654 | 0.4367 | 0.3273 |
| 26 | 2.00 | 2.02 | 0.0000 | 0.2266 | 0.7734 | 8.1550 | 1.8453 | 1.2622 | 0.4324 | 0.3022 |
| 27 | 2.02 | 2.04 | 0.0000 | 0.1972 | 0.8028 | 8.8123 | 1.8394 | 1.2593 | 0.4286 | 0.2799 |
| 28 | 2.04 | 2.06 | 0.0000 | 0.1710 | 0.8290 | 9.4954 | 1.8342 | 1.2568 | 0.4252 | 0.2600 |
| 29 | 2.06 | 2.08 | 0.0000 | 0.1475 | 0.8525 | 10.2042 | 1.8295 | 1.2546 | 0.4221 | 0.2421 |
| 30 | 2.08 | 2.10 | 0.0000 | 0.1264 | 0.8736 | 10.9388 | 1.8253 | 1.2524 | 0.4194 | 0.2261 |
| 31 | 2.10 | 2.12 | 0.0000 | 0.1073 | 0.8927 | 11.6992 | 1.8215 | 1.2505 | 0.4169 | 0.2116 |
| 32 | 2.12 | 2.14 | 0.0000 | 0.0901 | 0.9099 | 12.4854 | 1.8180 | 1.2488 | 0.4147 | 0.1984 |
| 33 | 2.14 | 2.16 | 0.0000 | 0.0744 | 0.9256 | 13.2973 | 1.8149 | 1.2473 | 0.4127 | 0.1865 |
| 34 | 2.16 | 2.18 | 0.0000 | 0.0601 | 0.9399 | 14.1350 | 1.8120 | 1.2459 | 0.4108 | 0.1757 |
| 35 | 2.18 | 2.20 | 0.0000 | 0.0470 | 0.9530 | 14.9985 | 1.8094 | 1.2446 | 0.4091 | 0.1657 |